Solvent and Pressure Effects on the Motions of Encapsulated Guests: Tuning the Flexibility of a Supramolecular Host

Jeffrey S. Mugridge[a], Achim Zahl[b], Rudi van Eldik[b], Robert G. Bergman[a]*, Kenneth N. Raymond[a]*

[a] *Department of Chemistry, University of California, Berkeley and Chemical Science Division, Lawrence Berkeley National Laboratory, Berkeley, CA 94720-1460*

[b] *Inorganic Chemistry, Department of Chemistry and Pharmacy, University of Erlangen-Nuremberg, Egerlandstr. 1, 91058 Erlangen, Germany*

rbergman@berkeley.edu; raymond@socrates.berkeley.edu

DISCLAIMER: This document was prepared as an account of work sponsored by the United States Government. While this document is believed to contain correct information, neither the United States Government nor any agency thereof, nor the Regents of the University of California, nor any of their employees, makes any warranty, express or implied, or assumes any legal responsibility for the accuracy, completeness, or usefulness of any information, apparatus, product, or process disclosed, or represents that its use would not infringe privately owned rights. Reference herein to any specific commercial product, process, or service by its trade name, trademark, manufacturer, or otherwise, does not necessarily constitute or imply its endorsement, recommendation, or favoring by the United States Government or any agency thereof, or the Regents of the University of California. The views and opinions of authors expressed herein do not necessarily state or reflect those of the United States Government or any agency thereof or the Regents of the University of California.

FUNDING: This work has been supported by the Director, Office of Science, Office of Basic Energy Sciences, and the Division of Chemical Sciences, Geosciences, and Biosciences of the U.S. Department of Energy at LBNL under Contract No. DE-AC02-05CH11231 and an NSF predoctoral fellowship to J.S.M. The authors also gratefully acknowledge financial support from the Bavaria California Technology Center.

Abstract

The supramolecular host assembly $[Ga_4L_6]^{12-}$ (**1**; L = 1,5-bis[2,3-dihydroxybenzamido]naphthalene) contains a flexible, hydrophobic interior cavity that can encapsulate cationic guest molecules and catalyze a variety of chemical transformations. The Ph–CH_2 bond rotational barrier for encapsulated *ortho*-substituted benzyl phosphonium guest molecules is sensitive to the size and shape of the host interior space. Here we examine how changes in bulk solvent (water, methanol, or DMF) or applied pressure (up to 150 MPa) affect the rotational dynamics of encapsulated benzyl phosphonium guests, as a way to probe changes in host cavity size or flexibility. When host **1** is dissolved in organic solvents with large solvent internal pressures $(\partial U/\partial V)_T$, we find that the free energy barrier to Ph–CH_2 bond rotation increases by 1 – 2 kcal/mol, compared with aqueous solution. Likewise, when external pressure is applied to the host-guest complex in solution, the bond rotational rates for the encapsulated guests decrease. The magnitude of these rate changes and the volumes of activation obtained

using either solvent internal pressure or applied external pressure, are very similar. NOE distance measurements reveal shorter average host-guest distances (~0.3 Å) in organic versus aqueous solution. These experiments demonstrate that increasing solvent internal pressure or applied external pressure reduces the host cavity size or flexibility, resulting in more restricted motions for encapsulated guest molecules. Changing bulk solvent or external pressure might therefore be used to tune the physical properties or reactivity of guest molecules encapsulated in a flexible supramolecular host.

Solvent and Pressure Effects on the Motions of Encapsulated Guests: Tuning the Flexibility of a Supramolecular Host

Jeffrey S. Mugridge[a], Achim Zahl[b], Rudi van Eldik[b], Robert G. Bergman[a]*, Kenneth N. Raymond[a]*

[a] *Department of Chemistry, University of California, Berkeley and Chemical Science Division, Lawrence Berkeley National Laboratory, Berkeley, CA 94720-1460*

[b] *Inorganic Chemistry, Department of Chemistry and Pharmacy, University of Erlangen-Nuremberg, Egerlandstr. 1, 91058 Erlangen, Germany*

rbergman@berkeley.edu; raymond@socrates.berkeley.edu

Introduction

One of the ways in which biological enzymes catalyze chemical transformations with unrivaled rate accelerations and selectivity is by tightly binding target substrates in specific and reactive conformations at the enzyme active site. By carefully controlling substrate orientation and motion, enzymes can lower the entropy of activation for a chemical reaction, contributing to catalysis. For example, the ribosome catalyzes peptide bond formation with rate enhancements of 10^7 by precisely positioning substrates for reaction in the active site during peptidyl transfer and thereby lowering the entropy of activation.[1] Likewise, confinement of guest molecules within synthetic supramolecular hosts can restrict the available conformational space and lead to conformational changes, chemical transformations, and catalysis.[2–5] Synthetic supramolecular assemblies have not yet achieved nearly the same level of substrate control as observed in biological systems, but researchers are beginning to examine how encapsulated guests can be selected based on size and shape,[6] and how guest motions can be tuned and controlled by the host interior environment.[7] Here we show that encapsulated guest motions can be modulated by changing host cavity size or flexibility through changes in bulk solvent or applied external pressure. Using changes in solvent and pressure to vary the supramolecular environment may provide additional ways to fine tune the reactivity of encapsulated guest molecules.

The supramolecular host $[Ga_4L_6]^{12-}$ (**1**; Figure 1; L = 1,5-bis[2,3-dihydroxybenzamido]naphthalene) self-assembles from four Ga^{3+} metals and six naphthalene-based biscatecholamide ligands into a *T*-symmetric cluster in which the metal ions occupy the vertices and the ligands span the edges of the molecular tetrahedron.[8,9] The supramolecular assembly **1** has a well-defined, hydrophobic interior cavity that can encapsulate appropriately-sized monocationic or neutral guest molecules.[10–14] The host ligand framework is flexible: apertures between ligands expand and contract to accommodate guest exchange and the volume of the interior cavity ranges from 250 to 450 $Å^3$ in the solid state, depending on the encapsulated guest (Figure 1, right).[15–17] Host **1** can also catalyze a variety of chemical transformations with altered regio-, stereo- or enantioselectivities, and enzyme-like rate accelerations of up to 10^6.[18–26]

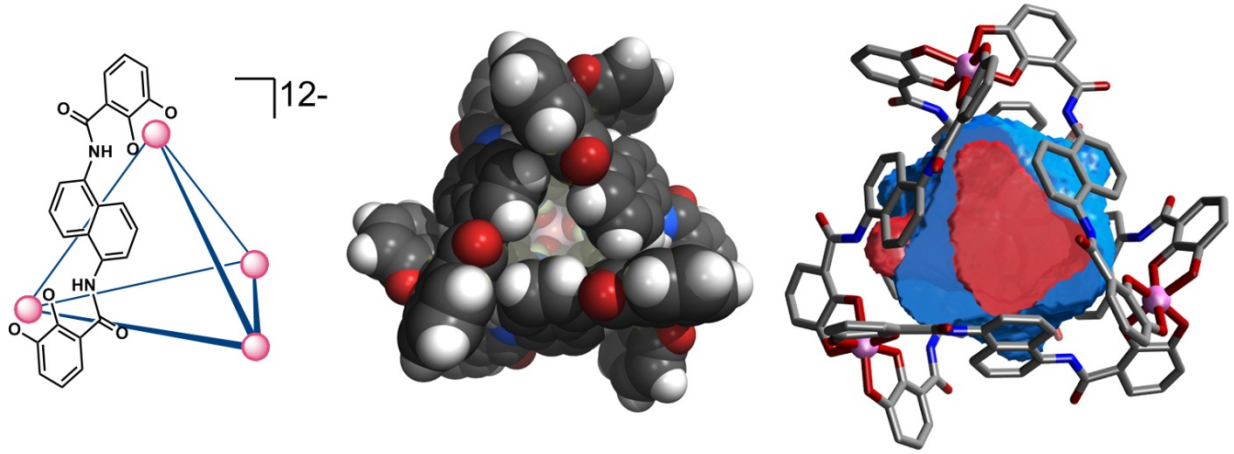

Figure 1. (Left) Schematic of supramolecular host **1** with only one ligand shown for clarity. (Middle) Space-filling representation of **1**, as viewed down one of the 3-fold symmetric host apertures. (Right) Wire frame model of **1** surrounding cutaway cavity void volumes for the smaller guest NEt_4^+ (red, cavity volume = 250 $Å^3$) and the larger guest decamethylcobaltocenium (blue, cavity volume = 450 $Å^3$).[17] The large variation in the size and shape of these cavities illustrates the flexibility of the host ligand framework.

We recently examined how encapsulation within host **1** affects guest motional dynamics by measuring the bond rotational barriers and tumbling behavior for a series of *ortho*-substituted benzyltrimethyl phosphonium guest molecules (**2** – **5**, Chart 1) encapsulated in **1**.[27] These studies found that upon encapsulation the guest Ph–CH_2 bond rotational barrier increased by 3 – 6 kcal/mol, reflecting the steric confinement imposed by encapsulation. Furthermore, guest rotational and tumbling dynamics were found to strongly depend on the size and shape of the guest and/or host cavity: generally, smaller and more prolate guest molecules had slower rotational and tumbling dynamics, while larger and more spherical guest molecules were able to move more freely within **1**. These experiments showed that despite the flexibility of the supramoelcular ligand framework, encapsulation imposes significant steric constraints on encapsulated guests and that guest internal motions are very sensitive to the supramolecular environment.

Chart 1. Benzyltrimethyl phosphonium guests **2** – **5**.

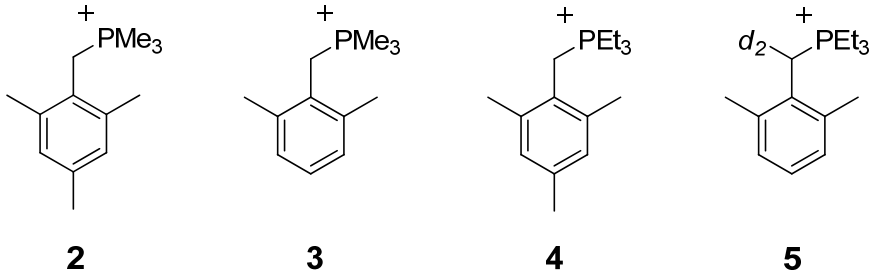

Based on these observations, we hypothesized that we could use Ph–CH_2 bond rotational barriers as a probe to quantitatively measure and understand subtle changes in the size or rigidity of the host ligand framework. Here, we examine Ph–CH_2 bond rotational barriers for guests **2** – **5** encapsulated in host **1** in different solvent systems. The encapsulated guest internal rotational barriers are found to increase by 1 – 2 kcal/mol when the host-guest complex is dissolved in solvents with a higher internal pressure $(\partial U/\partial V)_T$. This observation prompted us to measure rotational barriers at elevated external pressures, which led to similar increases in guest rotational barriers as observed for changing solvent system. From these studies, we conclude that increases in solvent internal pressure or increases in applied external pressure, lead to a decrease in host cavity size and/or flexibility, which restricts encapsulated guest motions. This conclusion is further supported by quantitative NOE measurements that reveal changes in mean cavity size in different solvents. Altering physical parameters such as solvent or pressure may provide an additional and widely applicable method to affect the supramolecular environment and tune encapsulated guest reactivity.

Results & Discussion

Bulk solvent perturbs the encapsulated guest rotational barriers. Previously, we showed that in CD_3OD solution the Ph–CH_2 bond rotational barrier for guests **2** – **5** is raised by between 3 and 6 kcal/mol upon encapsulation in host **1** and that these encapsulated rotational barriers can be used to probe the steric environment of the host interior.[27] Host **1** is soluble in water, methanol, DMF and DMSO solvents, and we wanted to know if and how the dynamics of encapsulated guest molecules change in different solvent systems. These data might also inform catalysis and reactivity studies with **1**, since changes in encapsulated guest motions or host flexibility should impact the size and scope of substrates able to be encapsulated and undergo reaction within **1**, as well as potentially change product selectivities.

In the chiral environment of host **1**, the *ortho* methyl groups of guests **2** – **5** are chemically inequivalent if Ph–CH_2 bond rotation is slow on the NMR timescale. We used selective inversion recovery (SIR) NMR experiments[28] to measure the rate of exchange (k_{exch}) between these methyl groups, which is equivalent to Ph–CH_2 bond rotation, at different temperatures to obtain activation parameters for encapsulated guest bond rotation. The encapsulated Ph–CH_2 bond rotational barriers for guests **2** – **5** were measured in D_2O, CD_3OD and DMF–d_7 solvents (Table 1). While these host–guest complexes are also soluble in DMSO, overlapping peaks in the encapsulated guest region for several of the host–guest complexes prevented measurement of the Ph–CH_2 bond rotational barriers in DMSO solvent.

Table 1. Activation parameters for Ph–CH_2 bond rotation of phosphonium guest molecules encapsulated within host **1** in D_2O, CD_3OD and DMF–d_7 solution. Data in CD_3OD are repeated from reference 27.

Guest		Solvent	**$\Delta G^{\ddagger}$(rotation)**, 298 K (kcal/mol)	**$\Delta H^{\ddagger}$(rotation)** (kcal/mol)	**$\Delta S^{\ddagger}$(rotation)** (cal/mol K)
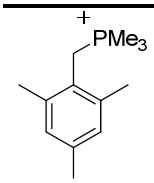	**2**	D_2O	17.2(1)	14.63(6)	–8.54(4)
		CD_3OD	19.1(5)	22.1(6)	10.0(3)
		DMF–d_7	19.2(4)	22.7(5)	11.6(3)
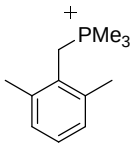	**3**	D_2O	15.3(6)	12.2(4)	–10.5(4)
		CD_3OD	17.1(1)	19.4(1)	7.80(5)
		DMF–d_7	17.7(6)	16.5(6)	–4.2(2)
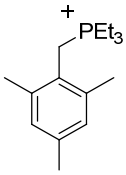	**4**	D_2O	16.7(3)	14.3(3)	–8.0(2)
		CD_3OD	17.3(4)	20.6(5)	11.1(3)
		DMF–d_7	18.0(2)	19.6(2)	5.46(8)
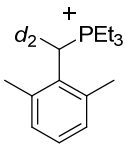	**5**	D_2O	15.4(2)	13.7(1)	–5.64(7)
		CD_3OD	16.3(1)	17.53(8)	4.35(2)
		DMF–d_7	16.8(4)	17.4(4)	2.24(6)

The trends in encapsulated rotational barriers as a function of guest size and shape that were previously observed in CD_3OD – the rotational barriers are dominated by enthalpic forces, decrease when PMe_3 groups are replaced by PEt_3 groups, and increase when a *para* methyl group is introduced – are preserved across each solvent. These size and shape effects are discussed in detail in our previous report on encapsulated guest rotational barriers.[27] A trend in the rotational barrier as a function of solvent is also observed: for each guest, moving from D_2O, to CD_3OD to DMF–d_7 increases the Ph–CH_2 bond rotational barriers by 1 – 2 kcal/mol. Although these are relatively small changes in free energy, it is the rate of encapsulated bond rotation (k_{exch}) that is actually measured in the SIR experiments and 1 or 2 kcal/mol in free energy corresponds to a significant and easily measurable change, about one order of magnitude, in the bond rotational rate (Figure 2). These experiments suggest that the motional space of encapsulated guest molecules is more restricted when the host–guest complex is dissolved in organic solution (methanol or DMF) than it is in aqueous solution.

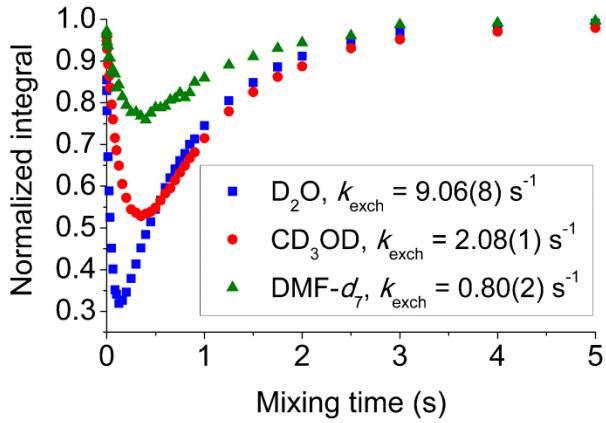

Figure 2. Plots of the normalized integral for an exchanging Ar–CH_3 resonance of guest **5** versus mixing time as measured by SIR NMR experiments at ~ 285 K in different solvents. The slower Ar-CH_3 rotational rates in organic solvents are reflected in the shallow exchange curves shown above. Data are shown for host–guest complexes of [**5** ⊂ **1**]$^{11-}$ in D_2O (at 283 K), CD_3OD (at 286 K) and DMF–d_7 (at 285 K); for all experiments [**1**] = 7 mM and [**5**] = 14 mM. k_{exch} is the observed rate constant for the exchange between encapsulated guest *ortho* methyl group NMR resonances, which is equivalent to Ph–CH_2 bond rotation.

Why are guest motions apparently restricted when the host–guest complex is dissolved in organic solution? One hypothesis is that the host framework is less flexible and/or the host cavity is slightly smaller in methanol and DMF than in water. A smaller mean cavity volume, or more rigid host movements (*e.g.* breathing modes), would lead to larger activation energies for encapsulated guest motions, both internal bond rotation and tumbling dynamics. Some support for this hypothesis comes from the observation that the bond rotational barriers for encapsulated guests trend with solvent internal pressure (P_i), which is defined as the change in internal energy of a solvent as it undergoes an infinitesimal isothermal volume expansion ($P_i = (\partial U/\partial V)_T$).[29,30] This parameter is governed mainly by dispersion or van der Waals interactions, rather than intermolecular interactions such as hydrogen bonding, so water has a very small internal pressure compared to most organic solvents. The internal pressure increases in moving from water to methanol to DMF (P_i = 151, 288, 480 MPa, respectively) and this roughly trends with the increase in bond rotational barriers observed in each solvent. It is possible that higher internal pressures may lead to a more rigid and compressed assembly framework and this could account for the apparent restriction of encapsulated guest motional dynamics in organic solvents. Solvent internal pressure was the only solvent parameter we found to trend well with these rotational rate data, other physical properties such as viscosity and dielectric constant were considered, but failed to mirror the observed trends in Ph–CH_2 rotational barriers.

It might alternatively be proposed that encapsulated guests are transiently solvated by small solvent molecules that are quickly moving in and out of the host apertures. The observed changes in rotational barrier would then be due to different molecular environments for the bound cation. Although encapsulated guests are typically thought to be fully desolvated from bulk solution, it is known that water can transiently enter the host cavity, even while other guests are present.[31] Evidence against this alternative is provided by experiments reported in our previous investigation of encapsulated rotational barriers, in which the Ph–CH_2 bond rotational barriers for an asymmetric derivative of **2** (**6**, Chart 2) were found to be the same within error in both methanol and 90% toluene / 10% methanol solutions at low temperatures.[27] Furthermore, to

directly address the question of electronic environment for the solvents at hand, the bond rotational barrier for cation **6** in bulk DMF–d_7 solution was measured by SIR NMR experiments and found to be 13(1) kcal/mol at 298 K. This is the same within error as the rotational barrier measured for **6** in bulk CD_3OD solution: 13.4(6) kcal/mol at 298 K. Thus, the Ph–CH_2 bond rotational barrier for cation **6** is invariant across three different solvents: methanol, DMF and toluene, demonstrating that transient contact with bulk solvent cannot be responsible for the observed changes in the rotational dynamics of guests encapsulated within **1**.

Chart 2. Asymmetric derivative of guest **2**, used for measurements in bulk solution.

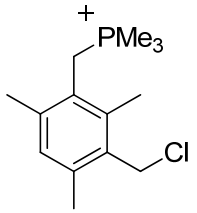

6

Applied pressure changes host flexibility and encapsulated guest dynamics. There is some ambiguity in the literature over whether solvent internal pressure and applied external pressure have similar effects on the reactivity and physical properties of molecules in solution. Both solvent internal pressure[32,33] and applied external pressure[34–36] can influence solution-state molecular conformations. In many cases, similar pressure effects on reaction rates have been measured using solvent internal pressure and applied external pressure.[37–40] However, the correlation between external and internal pressures is not always good,[41] possibly because changing solvent also dramatically alters many other important physical properties of the solution, such as the dielectric constant, viscosity and specific solute–solvent interactions. Supramolecular host **1** provides a unique system in which to test the equivalence of external and internal pressures, since the guest is isolated from bulk solvent and thus effects arising from changes in dielectric and solute-solvent interactions are minimized. In order to further explore the hypothesis that the observed solvent effects were due to changes in solvent internal pressure, the encapsulated Ph–CH_2 bond rotational rates were measured at elevated external pressures of up to 150 MPa (1500 atm). Encapsulated Ph–CH_2 rotational rates as a function of pressure in different solvents for guest **4** and **5** are listed below in Tables 2 and 3, and Figure 3 shows SIR data for $[\mathbf{5} \subset \mathbf{1}]^{11-}$ in DMF–d_7 at various applied pressures.[42]

Table 2. Ph–CH_2 bond rotational rates (k_{exch} is the observed rate constant for Ph–CH_2 bond rotation) for guest **4** encapsulated in host **1** in CD_3OD and DMF–d_7 solution at different external pressures.

Solvent	Temp (K)	k_{exch} (s^{-1}) at **5 MPa**	k_{exch} (s^{-1}) at **75 MPa**	k_{exch} (s^{-1}) at **150 MPa**
CD_3OD	298	1.22(4)	– [a]	0.63(4)
CD_3OD	308	2.70(9)	2.07(4)	1.35(4)
DMF–d_7	313	2.21(4)	1.21(2)	0.85(2)

[a] k_{exch} was not recorded at 75 MPa for guest **4** in CD_3OD at 298 K because the data recorded at 308 K were sufficient to establish the trend in Ph–CH_2 rotational rate with applied pressure and determine a volume of activation for this process. SIR data at 308 K were more robust due to the faster bond rotational rate at this temperature.

Table 3. Ph–CH_2 bond rotational rates (k_{exch} is the observed rate constant for Ph–CH_2 bond rotation) for guest **5** encapsulated in host **1** in D_2O, CD_3OD and DMF–d_7 solution at different external pressures.

Solvent	T (K)	k_{exch} (s^{-1}) at **5 MPa**	k_{exch} (s^{-1}) at **75 MPa**	k_{exch} (s^{-1}) at **150 MPa**
D_2O	294	23.7(7)	– [a]	21.4(9)
D_2O	285	11.6(2)	– [a]	10.7(2)
CD_3OD	298	9.4(2)	7.3(2)	5.5(1)
DMF–d_7	298	3.38(5)	2.22(3)	1.42(2)

[a] Data were not recorded at 75 MPa for guest **5** in D_2O because no change in encapsulated guest Ph–CH_2 rotational rate was seen between 5 and 150 MPa.

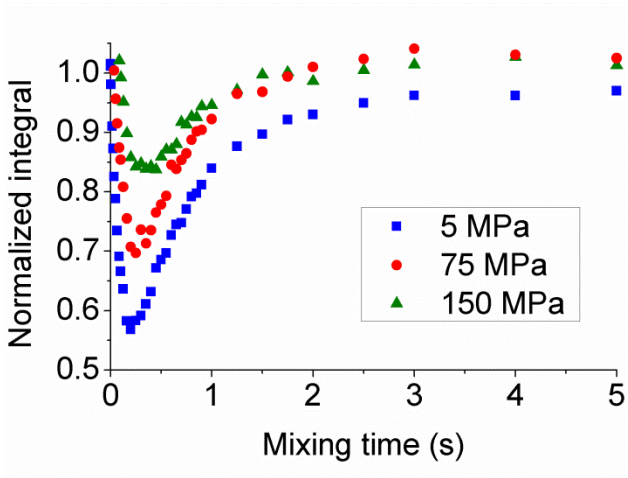

Figure 3. Plots of the normalized integral for an exchanging (via bond rotation) Ar–CH_3 resonance of guest **5** versus mixing time as measured by SIR NMR experiments at 298 K and different applied external pressures.

The above high–pressure NMR data show that the bond rotational rates of guest molecules **4** and **5** encapsulated in host **1** decrease with increasing external pressure in both CD_3OD and DMF–d_7 solvent. No pressure dependence on encapsulated bond rotation was observed for host–guest complexes in D_2O. In organic solvent, the bond rotational rates decrease by roughly a factor of two as the pressure is increased from 5 MPa to 150 MPa. This suggests a compression, or stiffening of the assembly framework as the external pressure is increased, leading to slower rotational dynamics for the encapsulated guest molecules.

The precise origin of the high pressure effects and the mechanism by which high pressure acts upon host **1** remain somewhat unclear. For example, solvent viscosity increases with increasing external pressure, and the magnitude of viscosity change at high pressures is larger for methanol and DMF than water, which mirrors the observed trend in encapsulated rotational rates.[43] However, when we examined the effects of viscosity changes on encapsulated Ph–CH_2 rotational rates by adding glycerol to the host-guest solution, we found that the magnitude of viscosity change induced by increasing applied pressure to 150 MPa would be much too small to account for the observed rate changes (see Supporting Information pages S15 – S16 for details). These data suggest that viscosity changes play a negligible role in determining the encapsulated rotational barriers at high pressure. We therefore cannot say that a single and specific physical property of the solvent is responsible for the rate changes at high pressure, only that increasing external pressure acts to shrink or rigidify the host cavity and slow encapsulated guest motional dynamics, and that the magnitude of this effect is very similar to that observed when changing solvent internal pressure.

The volume of activation ($\Delta V^{\ddagger}$; Equation 1), or the difference in molar volumes between the ground and transition state, can be derived from the pressure dependence on reaction rates.[44] The volumes of activation for encapsulated guest bond rotation range between 9 and 17 cm^3 mol^{-1} (Figure 4); this corresponds to an increase in the volume of the host–guest complex of between 15 and 30 $Å^3$ during bond rotation, a roughly 4 – 8 % increase relative to the host cavity volume for [**2** ⊂ **1**]$^{11-}$.[27] These activation volumes are similar in magnitude to those previously measured

for the guest exchange process from **1** in D_2O, which were found to be 13 cm^3 mol^{-1} for $NMe_2Pr_2^+$ and 31 cm^3 mol^{-1} for NPr_4^+.[16]

$$\Delta V^{\ddagger} = -RT\left(\frac{\partial \ln k}{\partial P}\right)_T \qquad \textbf{(Equation 1)}$$

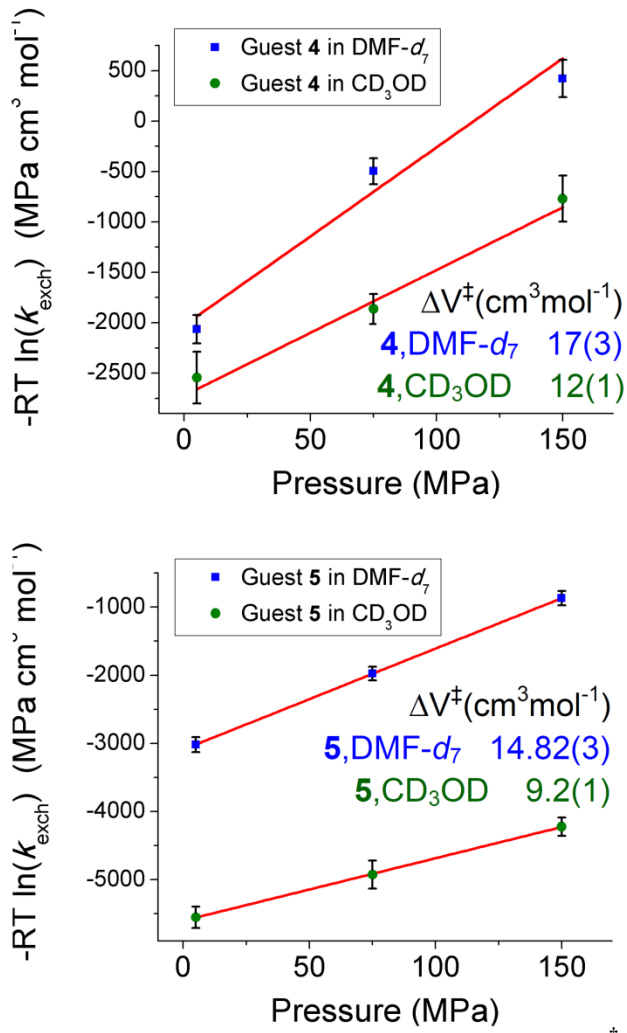

Figure 4. Plots used to determine the volumes of activation ($\Delta V^{\ddagger}$) for the Ph–CH_2 bond rotational processes for encapsulated guests **4** (top) and **5** (bottom); k_{exch} is the observed rate constant for Ph–CH_2 bond rotation and Pressure is the applied external pressure. High pressure measurements for guest **4** were carried out at 45 and 35 ºC in DMF-d_7 and CD_3OD, respectively (see Table 2). For guest **5**, high pressure measurements were carried out at 25 ºC in both DMF-d_7 and CD_3OD (see Table 3). Error bars are shown at three times the error on k_{exch}: the error on $RT\ln(k_{exch}) = RT(3\sigma_k/k_{exch})$, where σ_k is the error on the k_{exch} measurement shown in Tables 2 and 3.

Analogous activation volume plots for the encapsulated guest Ph–CH_2 bond rotational process can be constructed using rotational rates and solvent internal pressures (see Supporting Information, Figure S21). For guests **4** and **5**, the volumes of activation predicted from the solvent dependence of the rotational rate is about 17 cm^3 mol^{-1}; this is very consistent with the volumes of activation determined for these guests using applied external pressure (Figure 4). These data suggest that solvent internal pressure may indeed be responsible for the changes in encapsulated guest dynamics observed in different solvents, and that this effect may be analogous to the rate changes observed at high pressure. Therefore, supramolecular host **1** isolates the guest from bulk solvent, but appears to transmit both solvent internal and external pressure effects to the encapsulated guest, while minimizing the influence of changes in other solvent physical properties.

In summary, the effect of increasing external pressure or moving from aqueous to organic solution and thereby increasing solvent internal pressure, is to slow the Ph–CH_2 bond rotation of benzyl phosphonium guests encapsulated in host **1**. We observe good agreement between the effect of solvent internal pressure and applied external pressure on the encapsulated bond rotational rates, suggesting these two parameters have a similar effect on host **1**. Increasing the external or internal pressures is thought to compress or rigidify the host ligand framework and interior cavity, restricting the motional dynamics of encapsulated guest molecules.

Quantitative NOE distance measurements confirm changes in host size or flexibility. If host assembly **1** is more compressed and/or less flexible in solvents such as DMF–d_7 or CD_3OD, as compared to D_2O, the interior host cavity should have a smaller average volume in these organic solvents. Consequently, an encapsulated guest should spend on average more time closer to the interior naphthalene walls in a less flexible host (*e.g.* in DMF) than in a more flexible host (*e.g.* in D_2O). Quantitative nuclear Overhauser effect (NOE) NMR spectroscopy can be used to measure the through–space distance between protons with a high degree of precision.[45,46] Equation 2 relates a known distance (r_{AB}) to an unknown distance (r_{XY}) through the NOE growth rates (σ) of cross peaks in a 2D NOESY spectrum. The NOE has an r^{-6} distance dependence, making it very sensitive to small differences in nuclear separation. Thus, it should be possible to use NOE experiments to quantify small differences in the distance between an encapsulated guest and the host walls (Figure 6). Since encapsulated guests typically tumble rapidly on the NMR time scale,[47] any distance measurement will be an averaged value (averaged as r^{-6}), but this provides a quantitative measure to assess whether guests are on average closer to the host walls in different solvents.

$$r_{AB} = r_{XY}\left(\frac{\sigma_{XY}}{\sigma_{AB}}\right)^{\frac{1}{6}} \qquad \textbf{(Equation 2)}$$

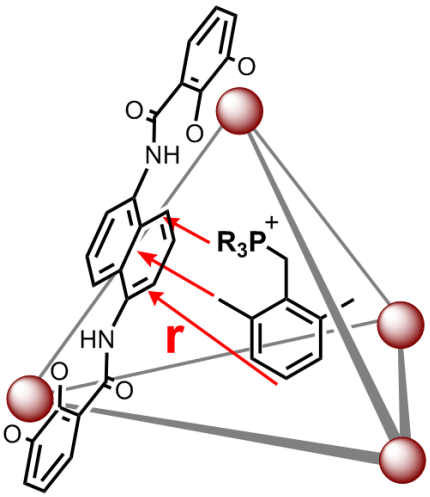

Figure 5. Schematic of host **1** with encapsulated guest showing distances between different guest and host moieties. Only one ligand is shown for clarity.

A series of 2D NOESY NMR spectra of the host–guest complex [**5** ⊂ **1**]$^{11-}$ were acquired at mixing times ranging from 0.01 – 1 second in both D_2O and DMF–d_7 solvents at 298 K. Guest **5** was chosen for this study because its internal–external exchange is very slow and the host–guest complex [**5** ⊂ **1**]$^{11-}$ is *T* symmetric at room temperature, simplifying the assignment of host–guest and host–host correlations (Figure 6). The NOE growth rates (σ) are extracted from the early portions (up to a mixing time of 0.2 seconds) of the mixing time versus intensity plots (Figure 7); according to the initial rate approximation, the NOE buildups at shorter mixing times are linear and depend only on internuclear separation. At longer mixing times, T_1 relaxation and secondary effects arising from large deviations from equilibrium spin populations, begin to compete with NOE buildup and the curves become non–linear.[48]

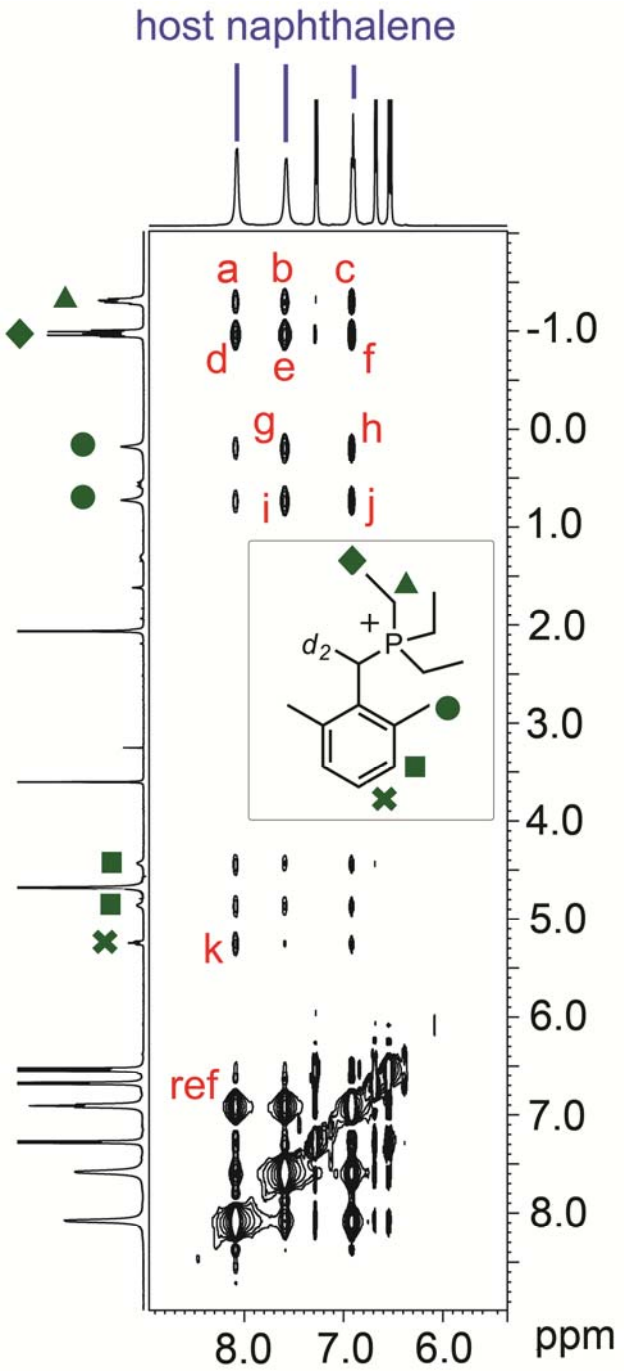

Figure 6. Portion of the 2D ^{1}H-^{1}H NOESY spectrum of [**5** ⊂ **1**]$^{11-}$ in D_2O at 298 K, mixing time = 0.5 sec. Encapsulated guest signals are labeled in green symbols, naphthalene host resonances are labeled with blue bars, and guest–naphthalene cross peaks used in the NOE distance analysis are labeled in red letters a – k ("ref" is the reference cross peak corresponding to *ortho*–naphthalene proton correlations). The inset shows the resonance assignments for encapsulated guest **5**.

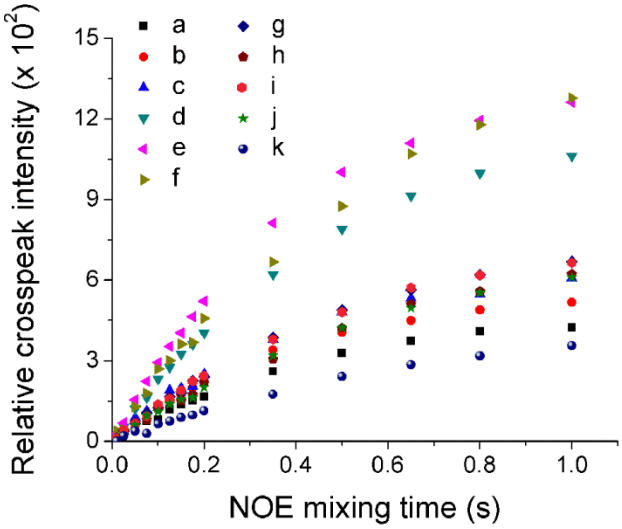

Figure 7. NOE buildup curves (0.01 – 1.0 seconds mixing time) for all analyzed host–guest correlations (a – k) of $[\mathbf{5} \subset \mathbf{1}]^{11-}$ in D_2O at 298 K. NOESY cross peak intensities for correlations a – k are reported relative to the reference cross peak (ref) at mixing time = 1 s. Positive NOE cross peaks, with respect to the diagonal cross peaks, are indicative of a large, slowly tumbling molecule.

The slopes of the linear portions of the NOE buildup curves give the initial NOE growth rates (σ), which are normalized according to the number of protons involved in each correlation (see Supporting Information pages S17 – S22 for details). Using the known *ortho* H–H distance (2.42 Å), equation 2 is applied to the normalized NOE growth rates to give the average host–guest distances, $\langle r \rangle$, for each correlation "a" – "k" in both D_2O and DMF–d_7. For each host–guest correlation measured, the average distance between guest **5** and host **1** is found to be roughly 0.3 Å shorter in DMF–d_7 than in D_2O solution (Table 4). This is consistent with the hypothesis that the host framework is more compressed and/or more rigid in DMF than in aqueous solution, and as a result the encapsulated guest spends on average more time closer to the host walls in the organic solvent. This is in contrast to D_2O solution, in which the ligand framework is more flexible and larger apparent host–guest distances are measured. Although these are fairly small distance differences, the validity of these measurements is strengthened by the facts that: (a) the same trend is observed across all of the host–guest correlations examined, and (b) the NOE distance measurement is very robust, owing to the r^{-6} distance dependence, and as such measured distances are relatively insensitive to inaccuracies in the growth rate.

Table 4. Average and differential host-guest distances measured for each **5** – **1** NOESY correlation in D_2O versus DMF–d_7. Errors on host-guest distances are derived from the standard error on the linear fit used to determine the NOE growth rate (σ) and listed here as three times the error on the measured distance.

Host–Guest correlation	Average host–guest distance in D_2O, $\langle r_{D2O} \rangle$ (Å)	Average host–guest distance in DMF-d_7, $\langle r_{DMF} \rangle$ (Å)	Difference in the average host–guest distances in DMF–d_7 vs. D_2O $\langle r_{D2O} \rangle - \langle r_{DMF} \rangle$ (Å)
A	5.52(8)	5.2(1)	**0.3(1)**
B	5.28(6)	4.99(8)	**0.3(1)**
C	5.2(1)	4.88(8)	**0.3(1)**
D	5.10(7)	4.86(5)	**0.24(9)**
E	4.90(6)	4.62(8)	**0.3(1)**
f	5.02(8)	4.69(6)	**0.3(1)**
g	4.63(6)	4.39(7)	**0.24(9)**
h	4.75(9)	4.43(8)	**0.3(1)**
i	4.63(6)	4.25(8)	**0.4(1)**
j	4.79(9)	4.45(6)	**0.3(1)**
k	4.39(9)	4.1(1)	**0.3(1)**

Conclusions

Our previous study on the motional dynamics of benzyl phosphonium guests confined within host **1** showed that the encapsulated bond rotational barriers were very sensitive to the size and shape of the host cavity.[27] Here, we used the Ph–CH_2 bond rotational barriers for encapsulated guests **2** – **5** to examine how bulk solvent and applied external pressure affect the flexibility and cavity size of host **1** and the internal motions of encapsulated guests. In the solvent effect studies, we found that when the host–guest complex was dissolved in D_2O, the measured bond rotational barriers were 1 – 2 kcal/mol lower than when the complex was dissolved in organic solution (CD_3OD or DMF–d_7). These free energy changes mirror the trend in solvent internal pressure – the bond rotational barrier increases in organic solvents where the internal pressure is greatest – which prompted us to examine the effect of externally applied pressure on encapsulated bond rotation. High–pressure NMR experiments showed decreases in the Ph–CH_2 bond rotational rates of encapsulated guests with increasing external pressures (up to 150 MPa) in organic solvent. The changes in bond rotational rates (2 – 10 fold) and the activation volumes (9 – 17 cm^3mol^{-1}) derived from solvent internal pressures were found to be very similar to those derived from applied external pressures, suggesting that increases in either solvent internal pressure or applied external pressure slows the motions of encapsulated guest molecules. Finally, NOE distance NMR measurements showed that the average guest–host distances were ~0.3 Å shorter in DMF–d_7 than in D_2O for encapsulated guest **5**. Therefore, the encapsulated guest spends more time closer to the host walls in DMF–d_7 than in D_2O and this suggests a more compressed or rigid host framework in organic solution that sterically restricts the motions of encapulsated guest molecules.

In summary, the motional dynamics of encapsulated guest molecules provide a remarkably sensitive probe of the host interior space. The bond rotational barriers measured for encapsulated guests in different solvents and at different applied pressures suggest that guests experience a confined steric environment within the host cavity and that this confinement is more severe in organic solvent and at elevated external pressures due to compression or rigidification of the host ligand framework. These features of guest encapsulation are important for understanding the changes in guest behavior that underlie both stabilization of reactive species and host–mediated catalysis.

Experimental

General. Unless otherwise noted, manipulations were carried out using standard Schlenk and glovebox techniques and all chemicals were obtained from commercial suppliers and used without further purification. All glassware was oven–dried at 150 °C. All solvents were sparged with nitrogen prior to use.

Host–Guest Complex Preparation. Supramolecular host assembly K_{11}[**1**],[49] and benzyl phosphonium molecules **2** – **6**,[27] were prepared as previously described and stored under nitrogen. All host–guest complexes were prepared *in situ* by mixing 1 equivalent of host K_{11}[**1**] with 2 equivalents of guest in either D_2O, CD_3OD or DMF–d_7 under a nitrogen atmosphere; the host–guest complexes were all formed quantitatively. For all host–guest complexes in CD_3OD and DMF–d_7, ~5% by volume DMSO–d_6 was added to the solution to aid host solubility. The internal pressure of DMSO is 512 MPa (larger than 480 MPa for DMF or 288 MPa for MeOH),

and so the 5% v/v addition of DMSO likely changes the internal pressures of both the DMF and methanol solutions by a small amount; however the 5% DMSO is constant across experiments in these solvents and should thus have little effect on interpretation of the solvent effect and high-pressure trends. Two equivalents of guest were used so that SIR experiments to measure the guest exchange kinetics (which require an exterior guest population) could be carried out on the same solution used to measure bond rotation. A host concentration of 7 mM was used for all rotational barrier measurements.

NMR Experimental Details. All ambient pressure selective inversion recovery (SIR) and 2D NOESY NMR experiments were carried out on a Bruker AV–500 NMR spectrometer. SIR NMR experiments to measure encapsulated guest Ph–CH_2 bond rotation were performed following previously described methods.[27] High–pressure NMR experiments (5 – 150 MPa) were carried out at the University of Erlangen-Nuremberg, Germany with a custom–built high–pressure NMR probe that fits into a standard, narrow-bore, Bruker AV–400 NMR spectrometer, as described.[50] The sample solution is placed in a standard 5mm NMR tube, cut to ~3", and sealed with a custom–made adjustable stopper. The temperature is adjusted with a recirculating water bath; temperature and pressure are allowed to fully equilibrate before data collection. For the NOE distance experiments, 2D ^{1}H-^{1}H NOESY spectra of [**5** ⊂ **1**]$^{11-}$ in D_2O at 298 K were collected at mixing times ranging 0.01 – 1.0 seconds. NOE growth rates (σ) are extracted from the slope of cross peak intensity versus mixing time plots, for each host-guest correlation of interest, and normalized according to the number of protons involved in each correlation. Normalized NOE growth rates for the host-guest correlations (a – k, unknown distances) and the normalized reference correlation NOE growth rate (ref, *ortho* H–H = 2.42 Å) are used in Equation 2 to compute the average host-guest distances.[45] See Supporting Information pages S17 – S25 for raw data and further details. All 2D ^{1}H-^{1}H NOESY spectra were analyzed in SPARKY.[51]

Acknowledgements. This work has been supported by the Director, Office of Science, Office of Basic Energy Sciences, and the Division of Chemical Sciences, Geosciences, and Biosciences of the U.S. Department of Energy at LBNL under Contract No. DE-AC02-05CH11231 and an NSF predoctoral fellowship to J.S.M. The authors also gratefully acknowledge financial support from the Bavaria California Technology Center.

Supporting Information Available: SIR fits and measured rate constants for guest bond rotation and exchange at ambient and elevated pressures, Eyring plots used to determine activation parameters for bond rotation, plots used to determine activation volumes for solvent internal pressure changes, and primary data for NOE distance analysis. This material is available free of charge via the internet at http://pubs.acs.org.

References

(1) Sievers, A.; Beringer, M.; Rodnina, M. V.; Wolfenden, R. *Proc. Natl. Acad. Sci. U.S.A.* **2004**, *101*, 7897–7901.

(2) Pluth, M. D.; Bergman, R. G.; Raymond, K. N. *Acc. Chem. Res.* **2009**, *42*, 1650–1659.

(3) Yoshizawa, M.; Klosterman, J. K.; Fujita, M. *Angew. Chem. Int. Ed.* **2009**, *48*, 3418–3438.

(4) Ajami, D.; Rebek, J. *Acc. Chem. Res.*, **2012**, doi: 10.1021/ar300038r.

(5) Laughrey, Z.; Gibb, B. C. *Chem. Soc. Rev.* **2010**, *40*, 363–386.

(6) For recent examples of size and shape selection in supramolecular systems, see: (a) Ronson, T. K.; Giri, C.; Kodiah Beyeh, N.; Minkkinen, A.; Topić, F.; Holstein, J. J.; Rissanen, K.; Nitschke, J. R. **2013**, *Chem. Eur. J.*, doi: 10.1002/chem.201203751. (b) Liao, P.; Langloss, B. W.; Johnson, A. M.; Knudsen, E. R.; Tham, F. S.; Julian, R. R.; Hooley, R. J. *Chem. Commun.* **2010**, *46*, 4932–4934. (c) Gan, H.; Gibb, B. C. *Chem. Commun.* **2012**, *48*, 1656–1658. (d) Jiang, W.; Ajami, D.; Rebek, J., Jr *J. Am. Chem. Soc.* **2012**, *134*, 8070–8073. (e) Dube, H.; Rebek, J., Jr *Angew. Chem. Int. Ed.* **2012**, *51*, 3207–3210. (f) Fang, Y.; Murase, T.; Sato, S.; Fujita, M. *J. Am. Chem. Soc.* **2013**, *135*, 613–615. (g) Takezawa, H.; Murase, T.; Fujita, M. *J. Am. Chem. Soc.* **2012**, *134*, 17420–17423.

(7) For recent examples of supramolecular control on guest motions, see: (a) Purse, B. W.; Butterfield, S. M.; Ballester, P.; Shivanyuk, A.; Rebek, J. *J. Org. Chem.* **2008**, *73*, 6480–6488. (b) Scarso, A.; Onagi, H.; Rebek, J. *J. Am. Chem. Soc.* **2004**, *126*, 12728–12729. (c) O'Leary, B. M.; Grotzfeld, R. M.; Rebek, J. *J. Am. Chem. Soc.* **1997**, *119*, 11701–11702. (d) Kurdistani, S. K.; Robbins, T. A.; Cram, D. J. *J. Chem. Soc., Chem. Commun.* **1995**, 1259–1260. (e) Kusukawa, T.; Yoshizawa, M.; Fujita, M. *Angew. Chem. Int. Ed.* **2001**, *40*, 1879–1884. (f) Vysotsky, M. O.; Pop, A.; Broda, F.; Thondorf, I.; Böhmer, V. *Chem.-Eur. J.* **2001**, *7*, 4403–4410. (g) Brouwer, E. B.; Enright, G. D.; Ratcliffe, C. I.; Facey, G. A.; Ripmeester, J. A. *J. Phys. Chem. B* **1999**, *103*, 10604–10616. (h) Chapman, R. G.; Sherman, J. C. *J. Org. Chem.* **2000**, *65*, 513–516. (i) Kitagawa, H.; Kobori, Y.; Yamanaka, M.; Yoza, K.; Kobayashi, K. *Proc. Natl. Acad. Sci. U.S.A.* **2009**, *106*, 10444–10448. (j) Kulasekharan, R.; Jayaraj, N.; Porel, M.; Choudhury, R.; Sundaresan, A. K.; Parthasarathy, A.; Ottaviani, M. F.; Jockusch, S.; Turro, N. J.; Ramamurthy, V. *Langmuir* **2010**, *26*, 6943–6953.

(8) Caulder, D. L.; Raymond, K. N. *Angew. Chem. Int. Ed.* **1997**, *36*, 1440–1442.

(9) Caulder, D. L.; Raymond, K. N. *Acc. Chem. Res.* **1999**, *32*, 975–982.

(10) Parac, T. N.; Caulder, D. L.; Raymond, K. N. *J. Am. Chem. Soc.* **1998**, *120*, 8003–8004.

(11) Parac, T. N.; Scherer, M.; Raymond, K. N. *Angew. Chem. Int. Ed.* **2000**, *39*, 1239–1242.

(12) Biros, S. M.; Bergman, R. G.; Raymond, K. N. *J. Am. Chem. Soc.* **2007**, *129*, 12094–12095.

(13) Hastings, C. J.; Pluth, M. D.; Biros, S. M.; Bergman, R. G.; Raymond, K. N. *Tetrahedron* **2008**, *64*, 8362–8367.

(14) Sgarlata, C.; Mugridge, J. S.; Pluth, M. D.; Tiedemann, B. E. F.; Zito, V.; Arena, G.; Raymond, K. N. *J. Am. Chem. Soc.* **2010**, *132*, 1005–1009.

(15) Davis, A. V.; Raymond, K. N. *J. Am. Chem. Soc.* **2005**, *127*, 7912–7919.

(16) Davis, A. V.; Fiedler, D.; Seeber, G.; Zahl, A.; van Eldik, R.; Raymond, K. N. *J. Am. Chem. Soc.* **2006**, *128*, 1324–1333.

(17) Pluth, M. D.; Johnson, D. W.; Szigethy, G.; Davis, A. V.; Teat, S. J.; Oliver, A. G.; Bergman, R. G.; Raymond, K. N. *Inorg. Chem.* **2009**, *48*, 111–120.

(18) Fiedler, D.; Bergman, R. G.; Raymond, K. N. *Angew. Chem. Int. Ed.* **2004**, *43*, 6748–6751.
(19) Leung, D. H.; Bergman, R. G.; Raymond, K. N. *J. Am. Chem. Soc.* **2006**, *128*, 9781–9797.
(20) Pluth, M. D.; Bergman, R. G.; Raymond, K. N. *Angew. Chem. Int. Ed.* **2007**, *46*, 8587–8589.
(21) Pluth, M. D.; Bergman, R. G.; Raymond, K. N. *Science* **2007**, *316*, 85–88.
(22) Brown, C. J.; Bergman, R. G.; Raymond, K. N. *J. Am. Chem. Soc.* **2009**, *131*, 17530–17531.
(23) Brown, C. J.; Miller, G. M.; Johnson, M. W.; Bergman, R. G.; Raymond, K. N. *J. Am. Chem. Soc.* **2011**, *133*, 11964–11966.
(24) Hastings, C. J.; Fiedler, D.; Bergman, R. G.; Raymond, K. N. *J. Am. Chem. Soc.* **2008**, *130*, 10977–10983.
(25) Hastings, C. J.; Pluth, M. D.; Bergman, R. G.; Raymond, K. N. *J. Am. Chem. Soc.* **2010**, *132*, 6938–6940.
(26) Wang, Z. J.; Brown, C. J.; Bergman, R. G.; Raymond, K. N.; Toste, F. D. *J. Am. Chem. Soc.* **2011**, *133*, 7358–7360.
(27) Mugridge, J. S.; Szigethy, G.; Bergman, R. G.; Raymond, K. N. *J. Am. Chem. Soc.* **2010**, *132*, 16256–16264.
(28) Bain, A. D.; Cramer, J. A. *J. Magn. Reson. A.* **1996**, *118*, 21–27.
(29) Reichardt, C. *Solvents and Solvent Effects in Organic Chemistry*; 3rd ed.; Wiley-VCH, 2003.
(30) Dack, M. R. J. *Chem. Soc. Rev.* **1975**, *4*, 211–229.
(31) Pluth, M. D.; Bergman, R. G.; Raymond, K. N. *J. Am. Chem. Soc.* **2008**, *130*, 11423–11429.
(32) Kruck, M.; Munoz, M. P.; Bishop, H. L.; Frost, C. G.; Chapman, C. J.; Kociok-Köhn, G.; Butts, C. P.; Lloyd-Jones, G. C. *Chemistry – A European Journal* **2008**, *14*, 7808–7812.
(33) Ouellette, R. J.; Williams, S. *J. Am. Chem. Soc.* **1971**, *93*, 466–471.
(34) Takaya, H.; Taniguchi, Y.; Wong, P. T. T.; Whalley, E. *The Journal of Chemical Physics* **1981**, *75*, 4823–4828.
(35) Taniguchi, Y.; Takaya, H.; Wong, P. T. T.; Whalley, E. *The Journal of Chemical Physics* **1981**, *75*, 4815–4822.
(36) McCarthy, A. N.; Grigera, J. R. *Journal of Molecular Graphics and Modelling* **2006**, *24*, 254–261.
(37) Drljaca, A.; Hubbard, C. D.; van Eldik, R.; Asano, T.; Basilevsky, M. V.; le Noble, W. J. *Chem. Rev.* **1998**, *98*, 2167–2290.
(38) Eckert, C. A. *Annu. Rev. Phys. Chem.* **1972**, *23*, 239–264.
(39) Tanko, J. M.; Suleman, N. K.; Hulvey, G. A.; Park, A.; Powers, J. E. *J. Am. Chem. Soc.* **1993**, *115*, 4520–4526.
(40) Neuman, R. C.; Gunderson, H. J. *J. Org. Chem.* **1992**, *57*, 1641–1643.
(41) Neuman, R. C. *J. Org. Chem.* **1972**, *37*, 495–496.
(42) For the high-pressure NMR experiments, Ph–CH_2 rotational rates, rather than activation energies, were measured and compared because the longer experiment times required with the lower sensitivity high-pressure NMR probe precluded full activation parameter determination.
(43) The correlation between viscosity and encapsulated bond rotational rates is exclusive to changes induced by high-pressures; as noted earlier, there is not a correlation between viscosity and bond rotational rates at ambient pressure.
(44) Van Eldik, R.; Asano, T.; Le Noble, W. J. *Chem. Rev.* **1989**, *89*, 549–688.
(45) Neuhaus, D.; Williamson, M. P. *The Nuclear Overhauser Effect in Structural and Conformational Analysis*; Wiley-VCH, 2000.
(46) Zuccaccia, C.; Bellachioma, G.; Cardaci, G.; Macchioni, A. *J. Am. Chem. Soc.* **2001**, *123*, 11020–11028.

(47) Encapsulated guest **5**, chosen for the NOE distance studies, tumbles rapidly on the NMR time scale within host **1** (the host exhibits *T* symmetry, as all ligands are chemically equivalent). The NOE distance measurements make the assumption that the correlation times for all of the involved nuclei are the same, which is true for a rigid, isotropically tumbling molecule. Although the host and guest are noncovalently bound, uniform correlation times should be a valid assumption since the host tumbles through solution on the ps – ns timescale, and the guest tumbles on the ~ms timescale. See Supporting Information pages S24 – S25 for details.
(48) Jacobsen, N. E. *NMR Spectroscopy Explained: Simplified Theory, Applications and Examples for Organic Chemistry and Structural Biology*; Wiley, 2007.
(49) Caulder, D. L.; Powers, R. E.; Parac, T. N.; Raymond, K. N. *Angew. Chem. Int. Ed.* **1998**, *37*, 1840–1843.
(50) Zahl, A.; Igel, P.; Weller, M.; van Eldik, R. *Rev. Sci. Instrum.* **2004**, *75*, 3152–3157.
(51) Goddard, T. D. and Kneller D. G., SPARKY 3, University of California, San Francisco.
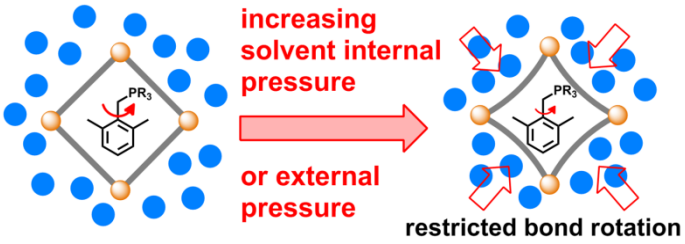
Table of Contents Graphic